

Casimir Energies in the Light of Renormalizable Quantum Field Theories¹

H. Weigel²

Institute for Theoretical Physics, Tübingen University
Auf der Morgenstelle 14, D-72076 Tübingen, Germany

Abstract

Effective hadron models commonly require the computation of functional determinants. In the static case these are one-loop vacuum polarization energies, known as Casimir energies. In this talk I will present general methods to efficiently compute renormalized one-loop vacuum polarization energies and energy densities and apply these methods to construct soliton solutions within a variational approach. This calculational method is particularly useful to study singular limits that emerge in the discussion of the *classical* Casimir problem which is usually posed as the response of a fluctuating quantum field to externally imposed boundary conditions.

Introduction

Many models in hadron physics originate from integrating out the more fundamental degrees of freedom like, for example, quarks. This change of field variables requires efficient tools to compute functional determinants like

$$\text{Det} (i\cancel{\partial} + \Gamma_i \Phi_i - m) , \quad (1)$$

in the Nambu–Jona–Lasinio model [1] for quark flavor dynamics [2]. Here Φ_i denote background fields that couple to the internal symmetries via the generators Γ_i . Functional determinants are highly ultraviolet divergent and thus need to be regularized, and eventually renormalized by perturbative counterterms. This is particularly elaborate when the perturbative expansions become invalid, as for example for soliton configurations [3]. These configurations are usually static, $\Phi_i(x) = \Phi_i(\vec{x})$, such that the determinant becomes proportional to the vacuum polarization energy

$$\frac{1}{2} \sum_n (\omega_n - \omega_n^{(0)}) . \quad (2)$$

Here ω_n are the eigenvalues of the single particle Hamiltonian in the presence of $\Phi_i(\vec{x})$ while $\omega_n^{(0)}$ denote the eigenvalues in the case that the Φ_i assume their vacuum values.

¹Talk presented at the 2nd intl. workshop *Effective Theories of Low Energy QCD*.

²Heisenberg–Fellow

In this talk I will describe tools to unambiguously regularize and renormalize such vacuum polarization energies and energy densities starting from the energy density operator in quantum field theory.

This presentation is based on work with E. Farhi, N. Graham, R. L. Jaffe, V. Khemani, M. Quandt, and M. Scandurra. The publications [4, 5, 6, 7, 8] of these collaborations should be consulted for further details.

Method

In quantum field theories energies and energy densities are computed as renormalized matrix elements of the energy density operator \hat{T}_{00} . Here I will present the method to unambiguously compute such a matrix element when the fluctuating quantum field is coupled to a classical background. The method is based on expressing this matrix element in terms of a Green's function with appropriate boundary conditions. Then the energy density is given by a sum over bound states plus an integral over the continuum scattering states. Ample use will be made of analytic properties of scattering data especially to deform momentum integrals along a cut on the positive imaginary axis. To regulate the ultraviolet divergences of the theory, which corresponds to eliminating the contribution associated with the semi-circle at infinite complex momenta, the leading Born approximations to the Green's function are subtracted and later exactly added back in as Feynman diagrams. These diagrams are then regularized and renormalized in ordinary Feynman perturbation theory.

Formalism

Consider a static, spherically symmetric background potential $\sigma = \sigma(r)$ with $r = |\vec{x}|$ in n spatial dimensions. The symmetric energy density operator for a real scalar field coupled to σ is

$$\hat{T}_{00}(x) = \frac{1}{2} \left[\dot{\phi}^2 + \phi \left(-\vec{\nabla}^2 + m^2 + \sigma(r) \right) \phi \right] + \frac{1}{4} \vec{\nabla}^2 (\phi^2) \quad (3)$$

with the spatial derivative term rearranged for later use of the Schrödinger equation to evaluate the expression in brackets. The “vacuum” is the state $|\Omega\rangle$ of lowest energy in the background σ . The “trivial vacuum” is the state $|0\rangle$ of lowest energy when $\sigma \equiv 0$. The vacuum energy density is the renormalized expectation value of \hat{T}_{00} with respect to the vacuum $|\Omega\rangle$, $\langle \Omega | \hat{T}_{00}(x) | \Omega \rangle_{\text{ren}}$, which includes the matrix elements of the counterterms. The energy density only depends on the radial coordinate r since σ spherically symmetric,

$$\epsilon(r) = \frac{2\pi^{n/2}}{\Gamma(\frac{n}{2})} r^{n-1} \langle \Omega | \hat{T}_{00}(x) | \Omega \rangle_{\text{ren}}. \quad (4)$$

The wavefunctions factorize in radial functions $\phi_\ell(t, r)$ and angle dependent spherical harmonics. The Fock decomposition for the radial functions reads

$$\begin{aligned} \phi_\ell(t, r) &= \frac{1}{r^{\frac{n-1}{2}}} \int_0^\infty \frac{dk}{\sqrt{\pi\omega}} \left[\psi_\ell(k, r) e^{-i\omega t} a_\ell(k) + \psi_\ell^*(k, r) e^{i\omega t} a_\ell^\dagger(k) \right] \\ &+ \frac{1}{r^{\frac{n-1}{2}}} \sum_j \frac{1}{\sqrt{2\omega_{\ell j}}} \left[\psi_{\ell j}(r) e^{-i\omega_{\ell j} t} a_{\ell j} + \psi_{\ell j}(r) e^{i\omega_{\ell j} t} a_{\ell j}^\dagger \right]. \end{aligned} \quad (5)$$

This decomposition contains scattering states with $\omega = \sqrt{k^2 + m^2}$ and bound states with $\omega_{\ell j} = \sqrt{m^2 - \kappa_{\ell j}^2}$. The total angular momentum assumes integer values $\ell = 0, 1, 2, \dots$ in all dimensions except for $n = 1$, where $\ell = 0$ and 1 only, corresponding to the symmetric and antisymmetric channels respectively. The radial wavefunctions ψ are solutions to the Schrödinger-like equation

$$-\psi'' + \frac{1}{r^2} \left(\nu - \frac{1}{2} \right) \left(\nu + \frac{1}{2} \right) \psi + \sigma(r)\psi - k^2\psi = 0 \quad (6)$$

where $\nu = \ell - 1 + \frac{n}{2}$. In each angular momentum channel, the wavefunctions are normalized to satisfy the completeness relation

$$\frac{2}{\pi} \int_0^\infty dk \psi_\ell^*(k, r) \psi_\ell(k, r') + \sum_j \psi_{\ell j}(r) \psi_{\ell j}(r') = \delta(r - r'). \quad (7)$$

Then the standard equal time commutation relations for the quantum field ϕ yield canonical commutation relations for the creation and annihilation operators, $[a_\ell(k), a_{\ell'}^\dagger(k')] = \delta(k - k')\delta_{\ell\ell'}$ and $[a_{\ell j}, a_{\ell' j'}^\dagger] = \delta_{jj'}\delta_{\ell\ell'}$. All other commutators vanish. The vacuum $|\Omega\rangle$ is annihilated by all of the $a_\ell(k)$ and $a_{\ell j}$. The matrix element (4) can now be computed by inserting eq. (5) into eq. (3):

$$\begin{aligned} \epsilon(r) &= \sum_\ell N_\ell \left[\int_0^\infty \frac{dk}{\pi} \omega \psi_\ell^*(k, r) \psi_\ell(k, r) + \sum_j \frac{\omega_j}{2} \psi_{\ell j}(r)^2 \right] \\ &+ \frac{1}{4} D_r \sum_\ell N_\ell \left[\int_0^\infty \frac{dk}{\pi \omega} \psi_\ell^*(k, r) \psi_\ell(k, r) + \sum_j \frac{1}{2\omega_{\ell j}} \psi_{\ell j}(r)^2 \right] - \epsilon^{(0)}(r) + \epsilon_{\text{CT}}(r). \end{aligned} \quad (8)$$

Here N_ℓ is the degeneracy factor, $D_r = \frac{\partial}{\partial r} \left(\frac{\partial}{\partial r} - \frac{n-1}{r} \right)$, $\epsilon_{\text{CT}}(r)$ is the counterterm contribution, and $\epsilon^{(0)}(r)$ indicates the subtraction of the energy density in the trivial vacuum.

The scattering state contribution is identified with the Green's function by defining the local spectral density

$$\rho_\ell(k, r) \equiv \frac{k}{i} G_\ell(r, r, k), \quad (9)$$

where

$$G_\ell(r, r', k) = -\frac{2}{\pi} \int_0^\infty dq \frac{\psi_\ell^*(q, r) \psi_\ell(q, r')}{(k + i\epsilon)^2 - q^2} - \sum_j \frac{\psi_{\ell j}(r) \psi_{\ell j}(r')}{k^2 + \kappa_{\ell j}^2}, \quad (10)$$

so that for real k

$$\psi_\ell^*(k, r) \psi_\ell(k, r) = \text{Im} \{ k G_\ell(r, r, k) \} = \text{Re} \{ \rho_\ell(k, r) \}. \quad (11)$$

The $i\epsilon$ prescription has been chosen so that this Green's function is meromorphic in the upper half-plane, with simple poles at the imaginary momenta $k = i\kappa_{\ell j}$ corresponding to bound states. For real k , the imaginary part of the Green's function at $r = r'$ is an odd function of k , while the real part is even. Hence eq. (8) can be expressed as a contour integral in the upper half-plane. The contribution from the semi-circular contour at large $|k|$ with $\text{Im}(k) \geq 0$ must be eliminated. Subtracting sufficiently many terms in the Born series from the Green's function yields a convergent integral. Then I add back exactly what I subtracted in the form of Feynman diagrams. The integrand (8) has a branch cut along the imaginary axis, $k \in [im, +i\infty]$, and simple poles at the bound state momenta

$k = i\kappa_j$. The corresponding residues cancel the explicit bound state contributions. The discontinuity along the cut is hence all what is left to be considered

$$\begin{aligned}\epsilon(r) &= -\sum_{\ell} N_{\ell} \int_m^{\infty} \frac{dt}{\pi} \sqrt{t^2 - m^2} \left[1 - \frac{1}{4(t^2 - m^2)} D_r \right] [\rho_{\ell}(it, r)]_N + \sum_{i=1}^N \epsilon_{\text{FD}}^{(i)}(r) + \epsilon_{\text{CT}}(r) \\ &\equiv \bar{\epsilon}(r) + \sum_{i=1}^N \epsilon_{\text{FD}}^{(i)}(r) + \epsilon_{\text{CT}}(r),\end{aligned}\quad (12)$$

where

$$\begin{aligned}[\rho_{\ell}(k, r)]_N &\equiv \rho_{\ell}(k, r) - \rho_{\ell}^{(0)}(k, r) - \rho_{\ell}^{(1)}(k, r) \dots - \rho_{\ell}^{(N)}(k, r) \\ &= \frac{k}{i} \left[G_{\ell}(r, r, k) - G_{\ell}^{(0)}(r, r, k) - G_{\ell}^{(1)}(r, r, k) - \dots - G_{\ell}^{(N)}(r, r, k) \right].\end{aligned}\quad (13)$$

The superscript (j) indicates the term of order j in the Born expansion. Subtraction of the free Green's function $G_{\ell}^{(0)}(r, r, k)$ corresponds to subtracting $\epsilon^{(0)}(r)$ above. The potentially divergent pieces are precisely identified [9, 10] with Feynman diagrams $\epsilon_{\text{FD}}^{(i)}(r)$, which are regularized and renormalized using standard methods. When combined with the contribution from the counterterms $\epsilon_{\text{CT}}(r)$ they yield finite contributions to the energy density (for smooth backgrounds).

The Radial Green's Function

A variety of solutions to eq. (6) is distinguished by different boundary conditions:

free Jost solution	$w_{\ell}(kr)$:	$(-1)^{\nu} \sqrt{\frac{\pi}{2} kr} [J_{\nu}(kr) + iY_{\nu}(kr)]$
Jost solution	$f_{\ell}(k, r)$:	$\lim_{r \rightarrow \infty} \frac{f_{\ell}(k, r)}{w_{\ell}(kr)} = 1$
regular solution	$\phi_{\ell}(k, r)$:	$\lim_{r \rightarrow 0} \frac{\Gamma(\nu+1)}{\sqrt{\pi}} \left(\frac{r}{2}\right)^{-(\nu+\frac{1}{2})} \phi_{\ell}(k, r) = 1$
physical scattering solution	$\psi_{\ell}(k, r)$:	$\psi_{\ell}(k, r) = \frac{k^{\nu+\frac{1}{2}}}{F_{\ell}(k)} \phi_{\ell}(k, r)$.

The physical scattering solution is normalized with respect to the Jost function, $F_{\ell}(k)$ that is obtained as the ratio of the interacting and free Jost solutions at $r = 0$,

$$F_{\ell}(k) = \lim_{r \rightarrow 0} \frac{f_{\ell}(k, r)}{w_{\ell}(kr)}. \quad (14)$$

In particular, two regular solutions emerge: ϕ_{ℓ} has a simple boundary condition at $r = 0$, so that it is analytic in the upper half k -plane; ψ_{ℓ} has a physical boundary condition at $r \rightarrow \infty$, corresponding to incoming and outgoing spherical waves.

The Green's function has the simple representation

$$G_{\ell}(r, r', k) = \frac{\phi_{\ell}(k, r_{<}) f_{\ell}(k, r_{>})}{F_{\ell}(k)} (-k)^{\nu-\frac{1}{2}}, \quad (15)$$

where $r_{>}$ ($r_{<}$) denotes the larger (smaller) of the two arguments r and r' . The poles of $G_{\ell}(r, r', k)$ occur at the zeros of the Jost function, which are the imaginary bound state momenta. These are the only poles of eq. (10) in the upper half-plane and, since the

two functions in eq. (10) and eq. (15) obey the same inhomogeneous differential equation, they are indeed identical.

Although G_ℓ is analytic in the upper half-plane, f_ℓ and ϕ_ℓ contain pieces that oscillate for real k and exponentially increase or decrease when k has an imaginary part. Actually, only the case $r = r'$ is interesting, *cf.* eq. (13). Then the product $f_\ell\phi_\ell$ is well-behaved. This motivates to factorize the dangerous exponential components³,

$$f_\ell(k, r) \equiv w_\ell(kr)g_\ell(k, r) \quad \text{and} \quad \phi_\ell(k, r) \equiv \frac{(-k)^{-\nu+\frac{1}{2}} h_\ell(k, r)}{2\nu w_\ell(kr)}, \quad (16)$$

where w_ℓ is the free Jost solution introduced above. With these definitions,

$$G_\ell(r, r, k) = \frac{h_\ell(k, r)g_\ell(k, r)}{2\nu g_\ell(k, 0)}. \quad (17)$$

The definition of h_ℓ does *not* just remove the free part. Instead, it enforces the cancellation of w_ℓ in the Green's function. After analytically continuing to $k = it$, $g_\ell(it, r)$ obeys

$$g_\ell''(it, r) = 2t\xi_\ell(tr)g_\ell'(it, r) + \sigma(r)g_\ell(it, r) \quad (18)$$

with the boundary conditions $\lim_{r \rightarrow \infty} g_\ell(it, r) = 1$ and $\lim_{r \rightarrow \infty} g_\ell'(it, r) = 0$. A prime indicates a derivative with respect to the radial coordinate r . Using these boundary conditions, one integrates the differential equation numerically for $g_\ell(it, r)$, starting at $r = \infty$ and proceeding to $r = 0$. Similarly, $h_\ell(it, r)$ obeys

$$h_\ell''(it, r) = -2t\xi_\ell(tr)h_\ell'(it, r) + \left[\sigma(r) - 2t^2 \frac{d\xi_\ell(\tau)}{d\tau} \Big|_{\tau=tr} \right] h_\ell(it, r). \quad (19)$$

The factors in eq. (16) were chosen to yield simple boundary conditions: $h_\ell(it, 0) = 0$ and $h_\ell'(it, 0) = 1$. The numerical integration for h starts at $r = 0$ and runs to $r = \infty$. For real τ ,

$$\xi_\ell(\tau) \equiv -\frac{d}{d\tau} \ln [w_\ell(i\tau)] \quad (20)$$

is real with $\lim_{\tau \rightarrow \infty} \xi_\ell(\tau) = 1$, so the two functions $h_\ell(it, r)$ and $g_\ell(it, r)$ are manifestly real. They are also holomorphic in the upper half k -plane and, most importantly, they are bounded according to $|g_\ell(k, r)| \leq \text{const.}$ and $|h_\ell(k, r)| \leq \text{const.}_{[\nu r/(1+|k|r)]}$. Thus the representation of the partial wave Green's function in terms of g_ℓ and h_ℓ is smooth and numerically tractable on the positive imaginary axis.

The computation of the Born series, eq. (13), is also straightforward in this formalism. The solutions to the differential equations eq. (18) and eq. (19) are expanded about the free solutions,

$$\begin{aligned} g_\ell(it, r) &= 1 + g_\ell^{(1)}(it, r) + g_\ell^{(2)}(it, r) + \dots \\ h_\ell(it, r) &= 2\nu r I_\nu(tr) K_\nu(tr) + h_\ell^{(1)}(it, r) + h_\ell^{(2)}(it, r) + \dots, \end{aligned} \quad (21)$$

where the superscript labels the order of the background potential σ . The higher order components obey inhomogeneous linear differential equations such that σ is the source

³For $n = 1$ and $n = 2$, the case of $\ell = 0$ is somewhat different [5].

term for $g^{(1)}$, $\sigma g^{(1)}$ is the source term for $g^{(2)}$, and so on. Substituting these solutions in the expansion of eq. (17) with respect to the order of the background potential finally yields the Born series for the local spectral density

$$[\rho_\ell(it, r)]_N = \left[t \frac{h_\ell(it, r) g_\ell(it, r)}{2\nu g_\ell(it, 0)} \right]_N. \quad (22)$$

Thus I have available a computationally robust representation for the Born subtracted energy density $\bar{\epsilon}(r)$, *cf.* eq. (12).

Feynman Diagram Contribution

To one-loop order, the Feynman diagrams of interest are generated by expanding

$$\langle 0 | \hat{T}_{00}(x) | 0 \rangle \sim \frac{i}{2} \text{Tr} \left[\hat{T}_x \left(-\partial^2 - m^2 - \sigma \right)^{-1} \right] \quad (23)$$

to order N in the background σ . Here \hat{T}_x is the coordinate space operator corresponding to the insertion of the energy density defined by eq. (3) at the spacetime point x , and the trace includes space-time integration. The Feynman diagrams are obtained in ordinary perturbation theory, thus the matrix element in eq. (23) is evaluated between the trivial vacuum state, which is annihilated by the plane wave annihilation operators. The energy density operator has pieces of order σ^0 and σ^1 : $\hat{T}_x = \hat{T}_x^{(0)} + \hat{T}_x^{(1)}$. The computation of its vacuum matrix element is most conveniently performed in momentum space. The relevant matrix elements are

$$\langle k' | \hat{T}_x^{(0)} | k \rangle = e^{i(k'-k)x} \left[k^{0'} k^0 + \vec{k}' \cdot \vec{k} + m^2 \right] \quad \text{and} \quad \langle k' | \hat{T}_x^{(1)} | k \rangle = \sigma(x) e^{i(k'-k)x}. \quad (24)$$

Here I will explicitly consider the contributions to $\langle 0 | \hat{T}_{00}(x) | 0 \rangle$ that are linear in σ . The first contribution of this order comes directly from $\hat{T}_x^{(1)}$

$$\frac{i}{2} \text{Tr} \left(\frac{1}{-\partial^2 - m^2} \hat{T}_x^{(1)} \right) = \frac{i}{2} \sigma(x) \int \frac{d^d k}{(2\pi)^d} \frac{1}{k^2 - m^2}. \quad (25)$$

This local contribution is ultraviolet divergent for $d = n + 1 \geq 2$. It is canceled identically by the counterterm in the no-tadpole renormalization scheme. An additional contribution at order σ originates from $\hat{T}_x^{(0)}$ and the first-order expansion of the propagator,

$$\frac{i}{2} \text{Tr} \left(\frac{1}{-\partial^2 - m^2} \hat{T}_x^{(0)} \frac{1}{-\partial^2 - m^2} \sigma \right). \quad (26)$$

At $\mathcal{O}(\sigma)$ the renormalized Feynman diagram contribution to the energy density becomes

$$\epsilon_{\text{FD}}^{(1)}(r) + \epsilon_{\text{CT}}(r) = C_d r^{n-1} \int \frac{d^{d-1} q}{(2\pi)^{d-1}} \tilde{\sigma}(\vec{q}) e^{i\vec{q}\cdot\vec{x}} \int_0^1 d\zeta \frac{\zeta(1-\zeta)\vec{q}^2}{[m^2 + \zeta(1-\zeta)\vec{q}^2]^{2-d/2}}, \quad (27)$$

with $C_d = 2\pi^{\frac{d-1}{2}} \Gamma(2-\frac{d}{2}) / [\Gamma(\frac{d-1}{2})(4\pi)^{d/2}]$ and $\tilde{\sigma}(q) = 2\pi\delta(q^0)\tilde{\sigma}(\vec{q})$ is the Fourier transform of the (time independent) background field. This piece is finite for $d = n < 4$ and does not contribute to the total energy because it vanishes when integrated over space. The extension to higher order Feynman diagrams is straightforward.

Total Energy

The total energy is simply the integrated energy density of eq. (12),

$$E[\sigma] = \int_0^\infty \epsilon(r) dr . \quad (28)$$

Both, the t integral and the sum over channels in eq. (12), are absolutely convergent. This is a consequence of deforming the momentum integral in the upper-half plane⁴. Thus the order of integration can be interchanged

$$E[\sigma] = - \sum_\ell N_\ell \int_m^\infty \frac{dt}{\pi} \sqrt{t^2 - m^2} \int_0^\infty dr [\rho_\ell(it, r)]_N + \sum_{i=1}^N E_{\text{FD}}^{(i)} + E_{\text{CT}} , \quad (29)$$

where the total derivative term has integrated to zero. As already explained, a sufficient number, N , of Born approximations to the local spectral density $\rho_\ell(it, r)$ must be subtracted to render the t integral convergent. These subtractions are then added back in as the contribution to the total energy from the Feynman diagrams. Combined with the contribution from the counterterms this gives a finite result,

$$\sum_{i=1}^N E_{\text{FD}}^{(i)} + E_{\text{CT}} = \int_0^\infty dr \left[\sum_{i=1}^N \epsilon_{\text{FD}}^{(i)}(r) + \epsilon_{\text{CT}}(r) \right] . \quad (30)$$

In practice, $E[\sigma]$ is more efficiently computed directly from the perturbation series of the total energy. First, I'd like to recall that

$$2 \int_0^\infty dr [\rho(it, r)]_N = \frac{d}{dt} [\ln F_\ell(it)]_N = \frac{d}{dt} [\ln g_\ell(it, 0)]_N \quad (31)$$

is valid⁵ for $\text{Re}(t) > 0$, *cf.* Appendix A of Ref. [5]. This allows me to write

$$E[\sigma] = \sum_\ell N_\ell \int_m^\infty \frac{dt}{2\pi} \frac{t}{\sqrt{t^2 - m^2}} [\beta_\ell(t, 0)]_N + \sum_{i=1}^N E_{\text{FD}}^{(i)} + E_{\text{CT}} . \quad (32)$$

The real function $\beta_\ell(t, r) = \ln g_\ell(it, r)$ is determined by the differential equation

$$- \beta_\ell''(t, r) - [\beta_\ell'(t, r)]^2 + 2t\xi_\ell(tr)\beta_\ell'(k, r) + \sigma(r) = 0 \quad (33)$$

with the boundary conditions $\lim_{r \rightarrow \infty} \beta(t, r) = \lim_{r \rightarrow \infty} \beta'(t, r) = 0$. In $[\beta_\ell(t, 0)]_N$, the first N Born terms must again be subtracted. They are obtained by iterating the differential equation (33) according to the expansion of $\beta_\ell(t, r)$ in powers of σ .

To make contact with previous work [4, 6, 7, 10],

$$E[\sigma] = \sum_\ell N_\ell \left[\int_0^\infty \frac{dk}{2\pi} \sqrt{k^2 + m^2} \frac{d}{dk} [\delta_\ell(k)]_N + \frac{1}{2} \sum_j \omega_{\ell j} \right] + \sum_{i=1}^N E_{\text{FD}}^{(i)} + E_{\text{CT}} \quad (34)$$

⁴For real momenta, $k = it$, this amounts to performing the momentum integral before the radial integral.

⁵In general, the case $\text{Re}(t) = \text{Im}(k) = 0$ causes uncontrollable oscillations at large r : for real k the integral $\int_0^\infty dr [\rho(k, r)]_N$ does not exist and the integrated local spectral density cannot be related to the phase shift.

observe that along the real axis the phase of the Jost function is the scattering phase shift,

$$i \ln F_\ell(k) = i \ln |F_\ell(k)| + \delta_\ell(k). \quad (35)$$

Equations (32) and (34) are proven identical by first noticing that for real k $|F_\ell(k)|$ and $\delta_\ell(k)$ are respectively even and odd functions and then computing the momentum integrals along the branch cut $k \in [im, +i\infty]$.

Soliton Formation in a D=1+1 Chiral Model

The described method is well suited to efficiently and unambiguously compute vacuum polarization energies in renormalizable quantum field theories. Then the total energy, *i.e.* the sum of the classical and vacuum polarization energies, is a functional of the background field. Varying this background field maps an energy surface. The existence of a local minimum on that surface indicates the existence of an energetically stable solution to the equation of motion, a soliton⁶. Of particular interest are models that do not contain soliton solutions at the classical level such that solitons get stabilized by quantum corrections.

Now I would like to consider this idea in the framework of a simple chiral model in $D = 1+1$ [6]. The realistic $D = 3+1$ case is more difficult and a discussion is presented in Ref. [7]. In this two-dimensional model a two-component boson field $\vec{\phi} = (\phi_1, \phi_2)$ couples chirally to a fermion Ψ that come in N_f (equivalent) modes:

$$\mathcal{L} = \frac{1}{2} \partial_\mu \vec{\phi} \cdot \partial^\mu \vec{\phi} + \sum_{n=1}^{N_f} \bar{\Psi}_i \{i\cancel{\partial} - G(\phi_1 + i\gamma_5 \phi_2)\} \Psi_i. \quad (36)$$

where the potential for the boson field

$$V(\vec{\phi}) = \frac{\lambda}{8} \left[\vec{\phi} \cdot \vec{\phi} - v^2 + \frac{2\alpha v^2}{\lambda} \right]^2 - \alpha v^3 (\phi_1 - v) + \text{const}. \quad (37)$$

contains a term (proportional to α) that breaks the chiral symmetry explicitly in order to avoid problems stemming from (unphysical) infra-red singularities that occur when the vacuum configuration would be determined via the naïve treatment of spontaneous symmetry breaking[11]. In this manner it is guaranteed that the VEV is given by $\langle \vec{\phi} \rangle = (v, 0)$. Here the counterterm Lagrangian is not presented explicitly. It is determined such that the quantum corrections lead to a vanishing tadpole diagram for the boson field. Considering only the classical contribution does not support a stable soliton soliton.

In the limit that the number of fermion modes becomes large with $v^2/N_f \sim \mathcal{O}(1)$ only the classical and one fermion loop pieces contribute. In the following I will only consider that limit, *i.e.* $E_{\text{tot}} = E_{\text{cl}} + E_{\text{F}}$. The fermion contribution can be split into two pieces $E_{\text{F}} = E_{\text{vac}} + E_{\text{val}}$. The valence part E_{val} is given in terms of the bound state energies such as to saturate the total fermion number that is fixed to be N_{F} . The vacuum piece is computed according to the formalism described in the preceding section:

$$E_{\text{vac}}[\vec{\phi}] = -\frac{1}{2} \sum_i^{\text{b.s.}} (|\omega_i| - Gv) - \int_0^\infty \frac{dk}{2\pi} (\omega_k - Gv) \frac{d}{dk} (\delta_{\text{F}}(k) - \delta^{(1)}(k)), \quad (38)$$

⁶The minimum itself is not necessarily a soliton because the space of variational parameters is limited and the exact soliton might have even lower energy.

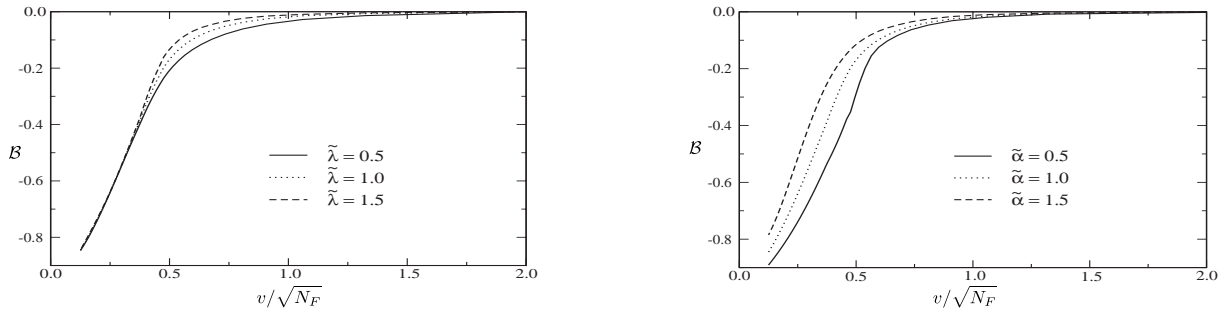


Figure 1: The maximal binding energy as a function of the model parameters as obtained from the *Ansatz* (40) in units of Gv ; $\tilde{\alpha} = \alpha/G^2$ and $\tilde{\lambda} = \lambda/G^2$.

which is obtained from Eq (34) by employing Levinson's theorem. Note the overall “-” sign for fermions and recall that the single particle spectrum is not charge conjugation invariant. Furthermore, δ_F denotes the sum of the eigenphase shifts⁷. The subtraction

$$\delta^{(1)}(k) = \frac{2G^2}{k} \int_0^\infty dx (v^2 - \vec{\phi}^2(x)) \quad (39)$$

that renders E_{vac} finite contains both first and second order Born approximants in the fluctuations of $\vec{\phi}$ about $\langle \vec{\phi} \rangle$. The first order is unambiguously fixed by the no-tadpole renormalization condition and the second order by the chiral symmetry.

Having established the energy functional I now consider variational *Ansätze* for the background field that turn this functional in a function of the variational parameters. As an example I assume

$$\phi_1 + i\phi_2 = v \{1 - R + R \exp [i\pi (1 + \tanh(Gvx/w))]\} \quad (40)$$

that introduces width (w) and amplitude (R) parameters. For prescribed model parameters ($G, v, \text{etc.}$) the energy must be minimized with respect to w and R . The resulting binding energy $\mathcal{B} = E_{\text{tot}} - Gv$ is shown in Fig. 1. Even though the *Ansatz* (40) may not be the final answer to the minimalization problem, \mathcal{B} is definitely negative. Thus a solitonic configuration is energetically favored showing that indeed quantum fluctuations can create a soliton that is not stable at the classical level.

Casimir energies

As noted earlier, the presented method to compute vacuum polarization energies is not limited to the case of smooth background fields. It is particularly interesting to employ singular background fields to imitate boundary conditions of the fluctuating quantum field. It is known for some time [12] that the vacuum polarization energy diverges when the fluctuating field is constrained by boundary conditions. *Ad hoc* schemes for their removal have been proposed [13]. However, the method of renormalization in continuum quantum field theory represents the *only* physical way to treat these divergences.

⁷The eigenchannels are labeled by parity and the sign of the single particle eigenenergies.

Dirichlet Points in One Space Dimension

The simplest example to be considered is that of a massive scalar field $\phi(t, x)$ in one dimension, constrained to vanish at $x = -a$ and a . The standard approach, in which the boundary conditions are imposed *a priori*, gives an energy [14]

$$\tilde{E}_2(a) = -\frac{m}{2} - \frac{2a}{\pi} \int_m^\infty dt \frac{\sqrt{t^2 - m^2}}{e^{4at} - 1}. \quad (41)$$

The tilde denotes the imposition of the Dirichlet boundary condition at the outset. This expression yields an attractive force between the two Dirichlet points,

$$\tilde{F}(a) = -\frac{d\tilde{E}_2}{d(2a)} = -\int_m^\infty \frac{dt}{\pi} \frac{t^2}{\sqrt{t^2 - m^2}(e^{4at} - 1)}. \quad (42)$$

In the massless limit it simplifies considerably: $\tilde{E}_2(a) = -\pi/48a$ and $\tilde{F}(a) = -\pi/96a^2$. But this result is not internally consistent: as $a \rightarrow \infty$, $\tilde{E}_2(a) \rightarrow 0$, indicating that the energy of an isolated ‘‘Dirichlet point’’ is zero. The limit $a \rightarrow 0$ also describes a single Dirichlet point, but $\tilde{E}_2(a) \rightarrow \infty$ as $a \rightarrow 0$. Also note that $\tilde{E}_2(a)$ is well defined as $m \rightarrow 0$, even though scalar field theories in one space dimension become infrared divergent when $m \rightarrow 0$.

The Dirichlet point problem can nicely be studied with the presented method. A single delta-function background

$$\sigma_1 = \lambda\delta(x - a) \quad (43)$$

has the Green’s function

$$G_\lambda(x, y) = G_0(x, y) - \frac{\lambda G_0(x, a)G_0(a, y)}{1 + \lambda G_0(a, a)} \quad (44)$$

where $G_0(x, y)$ is the Green’s function in the non-interacting case. The momentum argument has been omitted. Obviously the limit $\lambda \rightarrow \infty$ gives Dirichlet boundary conditions, $G_\infty(x, a) = G_\infty(a, y) = 0$. The vacuum polarization energy associated with eq. (43) is [5]

$$E_1(\lambda) = \int_m^\infty \frac{dt}{2\pi} \frac{t \ln \left[1 + \frac{\lambda}{2t} \right] - \frac{\lambda}{2}}{\sqrt{t^2 - m^2}} \quad (45)$$

To study the problem of two Dirichlet points it is obvious to consider

$$\sigma_2(x) = \lambda [\delta(x + a) + \delta(x - a)]. \quad (46)$$

The renormalized Casimir energy for this potential has also been computed in Ref. [5],

$$E_2(a, \lambda) = \int_m^\infty \frac{dt}{2\pi} \frac{1}{\sqrt{t^2 - m^2}} \left\{ t \ln \left[1 + \frac{\lambda}{t} + \frac{\lambda^2}{4t^2} (1 - e^{-4at}) \right] - \lambda \right\} \quad (47)$$

For any finite coupling λ , the inconsistencies noted in $\tilde{E}_2(a)$ do not afflict $E_2(a, \lambda)$: as $a \rightarrow \infty$, $E_2(a, \lambda) \rightarrow 2E_1(\lambda)$, and as $a \rightarrow 0$, $E_2(a, \lambda) \rightarrow E_1(2\lambda)$. Also $E_2(a, \lambda)$ diverges logarithmically in the limit $m \rightarrow 0$ as it should. The *force*, obtained by differentiating

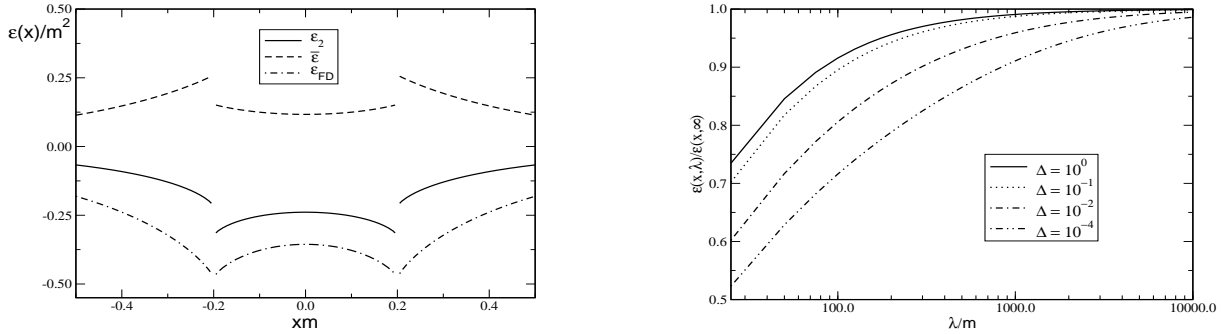


Figure 2: The energy density for the two delta function background at $a = 0.2/m$ computed from eqs (12) and (27). Left panel: $\lambda = 3m$. The distinct contributions associated with eqns. (12) and (27) are disentangled but the singular contributions at $x = \pm a$ are omitted. Right panel: Dirichlet limit $\lambda \rightarrow \infty$ in comparison to the the boundary condition result (48); $\Delta = (a - x)/a$.

eq. (47) with respect to $2a$, agrees with eq. (42) in the limit $\lambda \rightarrow \infty$. However $E_2(a, \lambda)$ *diverges* like $\lambda \log \lambda$ as $\lambda \rightarrow \infty$. Thus the renormalized Casimir *energy* diverges as the Dirichlet boundary condition is imposed, a physical effect which is missed in the pure boundary condition calculation.

The counterterms to the energy density vanish away from $x = \pm a$ because they are local functions of $\sigma(x)$. Therefore the Casimir *energy density* for $x \neq \pm a$ can be calculated assuming Dirichlet boundary conditions from the start simply by subtracting the density in the absence of boundaries without encountering any further divergences [14],

$$\begin{aligned} \tilde{\epsilon}_2(x, a) &= -\frac{m}{8a} - \int_m^\infty \frac{dt}{\pi} \frac{\sqrt{t^2 - m^2}}{e^{4at} - 1} - \frac{m^2}{4a} \sum_{n=1}^\infty \frac{\cos\left[\frac{n\pi}{a}(x-a)\right]}{\sqrt{\left(\frac{n\pi}{2a}\right)^2 + m^2}} \quad \text{for } |x| < a \\ \tilde{\epsilon}_2(x, a) &= -\frac{m^2}{2\pi} K_0(2m|x-a|) \quad \text{for } |x| > a. \end{aligned} \quad (48)$$

This result excludes the points $x = \pm a$. For finite λ the Casimir energy density, $\epsilon_2(x, a, \lambda)$, was also computed in Ref. [5] and is displayed in Fig. 2. The energy density between the isolated points is negative and approaches the boundary condition limit (48) in a non-uniform manner. In the limit $\lambda \rightarrow \infty$ it agrees with eq. (48) except at $x = \pm a$ where it contains extra, singular contributions. If one integrates eq. (48) over all x , ignoring the singularities at $x = \pm a$, one obtains eq. (41). Including the singular contributions at $\pm a$ by integrating $\epsilon_2(x, a, \lambda)$ gives eq. (47).

This simple example illustrates the principal situation: In the Dirichlet limit the renormalized Casimir energy diverges because the energy density on the “surface”, $x = \pm a$ diverges. However the Casimir force and the Casimir energy density for all $x \neq \pm a$ remain finite and equal to the results obtained by imposing the boundary conditions *a priori*, eqs. (42) and (48).

Two Space Dimensions

A scalar field in two space dimensions constrained to vanish on a circle of radius a presents a more complex problem. For smooth backgrounds only the local *tadpole* diagram diverges and thus the no-tadpole renormalization condition is still sufficient to render the theory

finite. For $\sigma(\vec{x}) = \lambda\delta(r - a)$ and $r \neq a$ the subtracted local spectral density $[\rho_\ell(it, r)]_0$ vanishes *exponentially* as the momentum along the cut in eq. (12) increases. For finite λ , both the t -integral and the ℓ -sum are uniformly convergent so $\lambda \rightarrow \infty$ can be taken under the sum and integral. The resulting energy density, $\epsilon(r, \lambda)$, agrees with $\tilde{\epsilon}(r)$, obtained when the Dirichlet boundary condition, $\phi(a) = 0$, is assumed from the start. As in one dimension, nothing can be said about the total energy because $\tilde{\epsilon}(r)$ is not defined at $r = a$, but unlike the one dimensional case, the integral $\int dr \epsilon(r, \lambda)$ now diverges even in the sharp limit for finite λ .

To understand the situation better, let's consider $\sigma(\vec{x})$ to be a narrow Gaussian of width w centered at $r = a$ and explore the sharp limit where $w \rightarrow 0$ and $\sigma(\vec{x}) \rightarrow \lambda\delta(r - a)$. For $w \neq 0$, σ does not vanish at any value of r , so $[\rho_\ell(it, r)]_0$ no longer falls exponentially at large t (and $r \neq a$), and subtraction of the first Born approximation to $\rho_\ell(it, r)$ is necessary, *i.e.* $N = 1$ in eq. (12). As noted above, the compensating tadpole graph can be canceled against the counterterm, $c_1\lambda\sigma(\vec{x})$. The result is a renormalized Casimir energy density, $\epsilon(r, w, \lambda)$, and Casimir energy, $E(w, \lambda) = \int_0^\infty dr \epsilon(r, w, \lambda)$, both of which are finite. However as $w \rightarrow 0$ both $\epsilon(a, w, \lambda)$ and $E(w, \lambda)$ diverge.

The divergence can be traced to the $\mathcal{O}(\lambda^2)$ Feynman diagram. This diagram is separated by subtracting the *second* Born approximation to $\rho_\ell(it, r)$, *i.e.* $N = 2$ in eq. (12). Then the ℓ -sum and t -integral no longer diverge in the sharp limit, $w \rightarrow 0$ but the equivalent diagram must be added back explicitly. In the limit $w \rightarrow 0$ it contributes

$$-\frac{\lambda^2 a^2}{8} \int_0^M dp J_0^2(ap) \arctan \frac{p}{2m} \quad (49)$$

to the total energy. This diverges logarithmically as $M \rightarrow \infty$. The divergence originates from the high momentum components in the Fourier transform of $\sigma(\vec{x}) = \lambda\delta(r - a)$ rather than the high energy behavior of the loop integral. This divergence gives an infinite contribution to the stress because it varies with the radius of the circle. This divergence only gets worse in higher dimensions (in contrast to the claim of Ref. [15]). For example, for $\sigma(r) = \lambda\delta(r - a)$ in three space dimensions the *renormalized* two point function is proportional to $\lambda^2 a^4 \int_0^M dp f(p)$ with $f(p) = p^2 j_0^2(pa) \ln p$ for large p . This integral diverges like $M \ln(M)$.

The imposed upper limit, M , in eq. (49) plays the role of a *physical* cutoff that regulates divergences localized on the surface. It is not related to the regulator of the ultraviolet divergences in loop integrals. Hence divergences like in eq. (49) are not renormalized by standard counterterms whose (divergent) coefficients are independent of the considered background because they are fixed by renormalization conditions on Green's functions at some prescribed finite external momenta. Divergences that emerge as $M \rightarrow \infty$ indicate that even the sharp limit $w \rightarrow 0$ does not exist. The strong coupling limit $\lambda \rightarrow \infty$ makes the divergence even worse. If the divergent terms depend on the quantity conjugate to the force (tension) under consideration⁸ the force (tension) cannot be defined independently of the structure of the material. This is the case for the shell or the sphere, but not for rigid bodies.

⁸For example, the distance between plates or the radius of the shell.

Conclusion

In this talk I have presented an efficient method to compute vacuum polarization energies in renormalizable quantum field theories for static background fields. Starting point for this method is the energy density operator. Its matrix element in the ground state is expressed in terms of the Green's function which subsequently is parameterized by data from scattering off the background field. To compute the momentum integrals as contour integrals in the upper-half plane, this approach makes ample use of the identity of Feynman diagrams and Born approximants to Casimir energies. More importantly, this identity allows one to implement standard (perturbative) renormalization conditions on the divergent, low order Green's functions. In this way the removal of the ultraviolet loop divergences is independent of the considered background.

Utilizing a variational approach to the so-obtained total energy, solitons can be constructed. As an application I have shown that in a 1+1 dimensional chiral model quantum corrections create a soliton that is classically unstable. In similar 3+1 dimensional models the situation is more complex [7], as issues like Landau poles [16] and sphaleron barriers [17] complicate matters.

The divergences that arise when a quantum field is forced to vanish on a surface can be nicely studied in this approach by implementing a boundary condition as the limit of a less singular background. Energy densities away from the surfaces or quantities like the force between rigid bodies, for which the surfaces can be held fixed, are finite and independent of the material cutoffs. Observables that require deformation or change in area of the surface cannot be defined independently of the other material properties.

Acknowledgments

I would like to thank the organizers for this interesting and worthwhile workshop. Furthermore I appreciate helpful remarks on the manuscript by M. Quandt and acknowledge support by the Deutsche Forschungsgemeinschaft (DFG) under contract We 1254/3-2.

References

- [1] Y. Nambu and G. Jona-Lasinio, Phys. Rev. **122** (1961) 345, **124** (1961) 246.
- [2] D. Ebert and H. Reinhardt, Nucl. Phys. B **271** (1986) 188.
- [3] R. Alkofer, H. Reinhardt, and H. Weigel, Phys. Rept. **265** (1996) 139.
- [4] For a comprehensive review see: N. Graham, R. L. Jaffe, and H. Weigel [arXiv:hep-th/0201148] in M. Bordag, ed., *Proceedings of the Fifth Workshop on Quantum Field Theory Under the Influence of External Conditions*, Intl. J. Mod. Phys. A **17** (2002) No. 6 & 7.
- [5] N. Graham, R. L. Jaffe, V. Khemani, M. Quandt, M. Scandurra, and H. Weigel, Nucl. Phys. B **645**, 49 (2002) [arXiv:hep-th/0207120].
- [6] E. Farhi, N. Graham, R. L. Jaffe, and H. Weigel, Phys. Lett. B **475**, 335 (2000) [arXiv:hep-th/9912283], Nucl. Phys. B **585**, 443 (2000) [arXiv:hep-th/0003144], Nucl. Phys. B **595** (2001) 536 [arXiv:hep-th/0007189], H. Weigel, arXiv:hep-th/0108180.
- [7] E. Farhi, N. Graham, R. L. Jaffe, and H. Weigel, Nucl. Phys. B **630**, 241 (2002) [arXiv:hep-th/0112217], E. Farhi, N. Graham, R. L. Jaffe, V. Khemani, and H. Weigel, *in preparation*.

- [8] N. Graham, R. L. Jaffe, V. Khemani, M. Quandt, M. Scandurra, and H. Weigel, arXiv:hep-th/0207205.
- [9] J. Schwinger, Phys. Rev. **94** (1954) 1362, J. Baacke, Z. Phys. C **53** (1992) 402.
- [10] E. Farhi, N. Graham, P. Haagensen, and R. L. Jaffe, Phys. Lett. B **427**, 334 (1998) [arXiv:hep-th/9802015], N. Graham and R. L. Jaffe, Nucl. Phys. B **544** (1999) 432 [arXiv:hep-th/9808140].
- [11] S. Coleman, Commun. Math. Phys. **31** (1973) 259.
- [12] D. Deutsch and P. Candelas, Phys. Rev. D **20** (1979) 3063, P. Candelas, Ann. Phys. **143** (1982) 241.
- [13] K. Symanzik, Nucl. Phys. B **190** (1981) 1, A. A. Actor, Ann. Phys. **230** (1994) 303, Fort. Phys. **43** (1995) 141.
- [14] V. M. Mostepanenko and N. N. Trunov, *The Casimir Effect and its Application*, Clarendon Press, Oxford (1997), K. A. Milton, *The Casimir Effect: Physical Manifestations Of Zero-Point Energy*, River Edge, USA: World Scientific (2001).
- [15] K. A. Milton, arXiv:hep-th/0210081.
- [16] G. Ripka and S. Kahana, Phys. Rev. D **36** (1987) 1233, J. Hartmann, F. Beck, and W. Benz, Phys. Rev. C **50** (1994) 3088. [arXiv:hep-ph/9410263].
- [17] G. 't Hooft, Phys. Rev. Lett. **37** (1976) 8, N. S. Manton, Phys. Rev. D **28** (1983) 2019, F. R. Klinkhamer and N. S. Manton, Phys. Rev. D **30** (1984) 2212.